

# Dark Matter Detectors as Dark Photon Helioscopes

Haipeng An,<sup>1</sup> Maxim Pospelov,<sup>1,2</sup> and Josef Pradler<sup>3</sup>

<sup>1</sup>*Perimeter Institute, Waterloo, Ontario N2L 2Y5, Canada*

<sup>2</sup>*Department of Physics and Astronomy, University of Victoria, Victoria, British Columbia V8P 5C2, Canada*

<sup>3</sup>*Department of Physics and Astronomy, Johns Hopkins University, Baltimore, Maryland 21210, USA*

(Received 23 April 2013; published 26 July 2013)

Light new particles with masses below 10 keV, often considered as a plausible extension of the standard model, will be emitted from the solar interior and can be detected on Earth with a variety of experimental tools. Here, we analyze the new “dark” vector state  $V$ , a massive vector boson mixed with the photon via an angle  $\kappa$ , that in the limit of the small mass  $m_V$  has its emission spectrum strongly peaked at low energies. Thus, we utilize the constraints on the atomic ionization rate imposed by the results of the XENON10 experiment to set the limit on the parameters of this model:  $\kappa \times m_V < 3 \times 10^{-12}$  eV. This makes low-threshold dark matter experiments the most sensitive dark vector helioscopes, as our result not only improves current experimental bounds from other searches by several orders of magnitude but also surpasses even the most stringent astrophysical and cosmological limits in a seven-decade-wide interval of  $m_V$ . We generalize this approach to other light exotic particles and set the most stringent direct constraints on “minicharged” particles.

DOI: [10.1103/PhysRevLett.111.041302](https://doi.org/10.1103/PhysRevLett.111.041302)

PACS numbers: 95.35.+d, 12.60.Cn, 96.60.Vg

**Introduction.**—The standard model (SM) of particle physics based on the gauge group structure  $G_{\text{SM}} = \text{SU}(3)_c \times \text{SU}(2)_L \times \text{U}(1)_Y$  and the Higgs mechanism is now firmly established and confirmed in a wide range of energies. At the same time, there are reasons to think that SM is an effective theory, and new ingredients must be added to it. New states may exist both at higher energy scales with sizable couplings to SM and at low energies where such states would have to be neutral under  $G_{\text{SM}}$  and very weakly coupled to the SM particles. Among the few distinct classes to couple new light states to the SM singlet operators, the  $\text{U}(1)_Y$  hypercharge field strength appears as the most natural [1]. It is singled out not only by its minimality but by its enhancement in the infrared (IR). The hypercharge portal leads to the mixing of an additional  $\text{U}(1)_V$  gauge boson (called “dark photon” from here on) with the SM photon, and thus can easily manifest itself in low-energy phenomena.

In the last few years, the model of kinetically mixed vectors has received tremendous attention, theoretically as well as experimentally. While the mass range above  $\sim 1$  MeV is mostly subjected to traditional particle physics constraints with high-intensity beams, the intermediate mass range, 10 eV to 1 MeV, is much constrained by astrophysics and cosmology. In the lowest mass range  $m_V < 10$  eV, astrophysical limits are complemented by direct laboratory searches of dark photons in nonaccelerator-type experiments. A collection of low-energy constraints on dark photons can be found in a recent review [2]. Among the most notable detection strategies are the “light-shining-through-the-wall” experiments (LSW) [3] and the conversion experiments from the solar dark photon flux, “helioscopes” [4]. The

latter class of experiments derives its sensitivity from the fact that such light vectors are readily excited in astrophysical environments, such as, e.g., in the solar interior, covering a wide range of masses up to  $m_V \sim \text{few keV}$ . Stellar astrophysics provides stringent constraints on any type of light, weakly interacting particles when the emission becomes kinematically possible [5]. Only in a handful of examples does the sensitivity of terrestrial experiments match the stellar energy loss constraints.

In a recent work [6], we have identified a new stellar energy loss mechanism originating from the resonant production of longitudinally polarized dark photons. Reference [6] significantly improved limits on dark photons compared to the original analysis [4], to the extent that all current LSW and helioscope experiments now find themselves deep inside astrophysically excluded regions.

The purpose of this Letter is to show that the newly calculated flux of dark photons in combination with the utmost sensitivity of direct dark matter detection experiments to atomic ionization make a powerful probe of dark photon models. In what follows, we calculate the solar flux of dark photons, both for the case of a “hard” Stueckelberg mass  $m_V$  and for a mass originating from breaking the  $\text{U}(1)_V$  through the Higgs mechanism. After that, we compute the atomic ionization rates from dark photons, taking full account of the medium effects, to derive powerful constraints on the parameter space of the model using the results of the XENON10 experiment.

**Dark photons.**—The minimal extension of the SM gauge group by an additional  $\text{U}(1)_V$  gauge factor yields the following effective Lagrangian well below the electroweak scale:

$$\mathcal{L} = -\frac{1}{4}F_{\mu\nu}^2 - \frac{1}{4}V_{\mu\nu}^2 - \frac{\kappa}{2}F_{\mu\nu}V^{\mu\nu} + \frac{m_V^2}{2}V_\mu V^\mu + eJ_{\text{EM}}^\mu A_\mu, \quad (1)$$

where  $V_\mu$  is the vector field associated with the Abelian factor  $U(1)_V$ . The field strengths of the photon  $F_{\mu\nu}$  and of the dark photon  $V_{\mu\nu}$  are connected via the kinetic mixing parameter  $\kappa$ , where a dependence on the weak mixing angle was absorbed;  $J_{\text{EM}}^\mu$  is the usual electromagnetic current with electric charge  $e$ .

Because of the  $U(1)$  nature of Eq. (1), we must distinguish two cases for the origin of  $m_V$ : the Stueckelberg case (SC) with nondynamical mass and the Higgs case (HC), where  $m_V$  originates through the spontaneous breaking of  $U(1)_V$ . In the latter case, Eq. (1) is extended by  $\mathcal{L}_\phi = |D_\mu \phi|^2 - V(\phi)$  with the dark Higgs field  $\phi = 1/\sqrt{2}(v' + h')$  in unitary gauge and after spontaneous symmetry breaking. The  $U(1)_V$  covariant derivative is  $D_\mu = \partial_\mu + ie'V_\mu$ , so that  $m_V = e'v'$ . The interactions between the physical field  $h'$  and  $V_\mu$  are given by

$$\mathcal{L}_{\text{int}} = e'm_V h' V_\mu^2 + \frac{1}{2}e'^2 h'^2 V_\mu^2. \quad (2)$$

The crucial difference between the two cases comes in the small  $m_V$  limit: while all processes of production or absorption of  $V$  in SC are suppressed,  $\Gamma_{\text{SC}} \sim O(m_V^2)$ , in HC there is no decoupling, and  $\Gamma_{\text{HC}} \sim O(m_V^0)$ . Indeed, in the limit  $m_{V,h'} \rightarrow 0$ , the  $V$ - $h'$  interaction with external electromagnetic (EM) charge is equivalent to the interaction of charged scalar field quanta with the effective EM charge of  $e_{\text{eff}} = \kappa e'$  [1,7]. Thus, the emission of particles from the  $U(1)_V$  sector is generically given by

$$\text{SC: } \gamma^{(*)} \rightarrow V; \quad \text{HC: } \gamma^{(*)} \rightarrow Vh', \quad (3)$$

where  $\gamma^{(*)}$  is any—virtual or real—photon. The ionization of an atom  $A$  in the detector can then be schematically described as

$$\text{SC: } V + A \rightarrow A^+ + e^-, \quad (4)$$

$$\text{HC: } V(h') + A \rightarrow h'(V) + A^+ + e^-, \quad (5)$$

where again all interactions are mediated by  $\gamma^{(*)}$ .

*Solar flux.*—The solar flux of dark photons in the SC is thoroughly calculated in Ref. [6]. In the small mass region,  $m_V \ll \omega_p$ , where  $\omega_p$  is the plasma frequency, the emission of longitudinal modes of  $V$  dominates the total flux, and the emission power of dark photons per volume can be approximated as

$$\frac{dP_L}{dV} \approx \frac{1}{4\pi} \frac{\kappa^2 m_V^2 \omega_p^3}{e^{\omega_p/T} - 1}. \quad (6)$$

For the purpose of this Letter, a more useful quantity is the energy-differential flux of dark photons at the location of

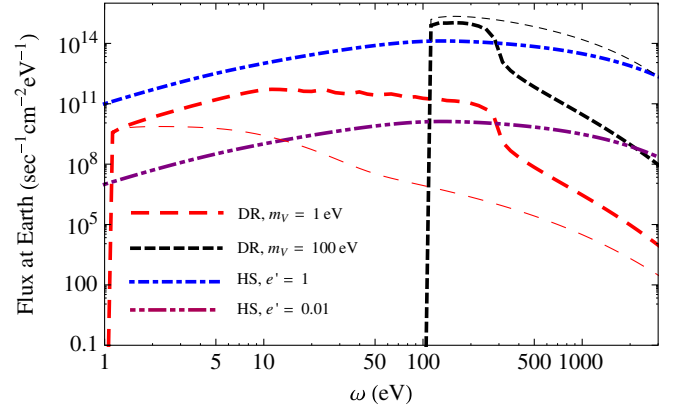


FIG. 1 (color online). Fluxes at Earth as functions of energy for both the SC and HC dark photons for  $\kappa = 10^{-12}$ . The thick long-dashed red and short-dashed black curves show the contribution from longitudinal dark radiation (DR) for  $m_V = 1$  and 100 eV, respectively. The corresponding thin curves show the transverse contribution. The one-dot-dashed blue and two-dot-dashed purple curves show the contribution from the HS process for  $e' = 1$  and 0.01, respectively.

Earth. The spectra for some representative values of the parameters are shown in Fig. 1.

We now turn to the HC: as already mentioned, in the small  $m_V$  region, the Higgs-strahlung process dominates the flux, whereas in the region where  $m_V$  is comparable to the plasma frequency inside the Sun,  $\omega_p = O(100 \text{ eV})$ , this process is subdominant due to phase space suppression. In vacuum, only an off-shell photon can convert to  $V$ . Inside a medium, however, the pole position is shifted and the  $\gamma^{(*)} \rightarrow V$  process is equivalent to the decay of either a “massive” transverse mode or a (longitudinal) plasmon. Inside the Sun, since transverse photons are more numerous than plasmons ( $\omega_p^3 \ll T^3$ ), the Higgs-strahlung process is dominated by the decay of transverse photons. The corresponding matrix element can be written as

$$\mathcal{M} = e'\kappa \epsilon_\mu^T(q)(k_1 - k_2)^\mu, \quad (7)$$

where  $k_1$  and  $k_2$  are the four-momenta of the outgoing dark Higgs particle,  $q = k_1 + k_2$  is the four-momentum of the decaying photon with transverse polarization vector  $\epsilon_\mu^T$ , and  $q^2 \approx \omega_p^2$ . Therefore, the total energy power density of dark radiation contributed by the Higgs-strahlung (HS) process can be estimated as

$$\left. \frac{dP}{dV} \right|_{\text{HS}} \approx \int \frac{d\Phi_2 d^3 \vec{q}}{2q^0 (2\pi)^3} \frac{2q^0}{e^{q^0/T} - 1} \overline{|\mathcal{M}|^2} = \frac{e_{\text{eff}}^2 \omega_p^5}{48\pi^3} f\left(\frac{\omega_p}{T}\right), \quad (8)$$

where  $d\Phi_2$  is the two-body phase space of the final state,  $\overline{|\mathcal{M}|^2}$  averages over the polarization of the transverse photons, and  $f(a) = \int_1^\infty dx (x^2 - 1)^{1/2} x / (e^{ax} - 1)$ . From the matrix element (7), we can also calculate the joint differential production rate of the dark vectors and Higgs particles, which can be written as

$$\left. \frac{d\Gamma^\phi}{dVd\omega} \right|_{\text{HS}} = \frac{e_{\text{eff}}^2 \omega_p^2}{4\pi^3} \int_{\omega + \omega_p^2/4}^{\infty} \frac{dq^0(\omega q^0 - \omega^2 - \omega_p^2/4)}{(e^{q^0/T} - 1)[(q^0)^2 - \omega_p^2]}. \quad (9)$$

It is important to note that for small  $m_V$  if medium effects restore the  $U(1)_V$  symmetry by driving  $v' \rightarrow 0$ , the Higgs-strahlung rate remains valid. The flux of dark photons on Earth in the HC for small  $m_{V(h')}$  is also shown in Fig. 1. As can be seen, the flux of  $V(h')$  is not enhanced in the IR but rather attains a broad maximum at dark photon energies  $\omega \sim 100$  eV.

*Absorption of dark photons.*—To calculate the absorption rate of dark photons in the detector's material (4), we need to know the photoelectric absorption cross section  $\sigma_{\text{abs}}$  and the index of refraction, encoded in the real and imaginary part of  $\epsilon_r$ , the relative permittivity of the target material.

In the SC, the amplitude for the absorption of a dark photon consists of the atomic transition matrix element multiplied by the propagator of  $\gamma^{(*)}$ . According to Ref. [6], it can be written as

$$\mathcal{M}_{i \rightarrow f + V_{T,L}} = -\frac{\kappa m_V^2}{m_V^2 - \Pi_{T,L}} \langle f | [e J_{\text{EM}}^\mu] | i \rangle \epsilon_\mu^{T,L}, \quad (10)$$

where  $\epsilon_\mu^{T,L}$  are the polarization vectors for the transverse and longitudinal modes of the dark photon ( $\epsilon_\mu^2 = -1$ ) and  $\Pi_{T,L}$  are defined via the polarization tensor inside the medium of the detector:

$$\Pi^{\mu\nu} \equiv e^2 \langle J_{\text{EM}}^{\mu\dagger}, J_{\text{EM}}^\nu \rangle = \Pi_T \sum_{i=1,2} \epsilon_i^{T\mu} \epsilon_i^{T\nu} + \Pi_L \epsilon^{L\mu} \epsilon^{L\nu}. \quad (11)$$

The total absorption rate can be written as

$$\Gamma_{T,L} = \frac{\kappa_{T,L}^2 e^2 \epsilon_\mu^{T,L*} \epsilon_\nu^{T,L}}{2\omega} \int d^4x e^{iq \cdot x} \langle i | J_{\text{EM}}^{\mu\dagger}(x) J_{\text{EM}}^\nu(0) | i \rangle, \quad (12)$$

where  $q$  is the dark photon four-momentum with  $\omega \equiv q^0$  and  $\kappa_{T,L}$  are the effective mixings for the transverse and longitudinal modes, respectively,

$$\kappa_{T,L}^2 = \frac{\kappa^2 m_V^4}{(m_V^2 - \text{Re}\Pi_{T,L})^2 + (\text{Im}\Pi_{T,L})^2}. \quad (13)$$

In Eq. (12), the correlation function should be taken in the physical region  $\omega > 0$ , where it is equal to  $-2 \text{Im}\langle J_{\text{EM}}^{\mu\dagger}, J_{\text{EM}}^\nu \rangle = e^{-2} \text{Im}\Pi^{\mu\nu}$  by unitarity (see, e.g., Ref. [8]). Therefore, the total absorption rate can be simplified to

$$\Gamma_{T,L} = -\frac{\kappa_{T,L}^2 \text{Im}\Pi_{T,L}}{\omega}. \quad (14)$$

Finally, in an isotropic nonmagnetic material, one has

$$\Pi_T = -\omega^2 \Delta\epsilon_r, \quad \Pi_L = -q^2 \Delta\epsilon_r, \quad (15)$$

where  $\Delta\epsilon_r \equiv \epsilon_r - 1$ . Combining Eqs. (13) and (14), we build the main formulas for the absorption rates of the transverse and longitudinal modes:

$$\Gamma_T = \left( \frac{\kappa^2 m_V^4 \text{Im}\epsilon_r}{\omega^3 |\Delta\epsilon_r|^2} \right) \left[ 1 + \frac{2m_V^2 \omega^2 \text{Re}\Delta\epsilon_r + m_V^4}{\omega^4 |\Delta\epsilon_r|^2} \right]^{-1},$$

$$\Gamma_L = \frac{\kappa^2 m_V^2 \text{Im}\epsilon_r}{\omega |\epsilon_r|^2}. \quad (16)$$

In general,  $\epsilon_r$  depends on both the injecting energy  $\omega$  and  $\vec{q}^2$ . The latter is suppressed by  $\sim \vec{q}^2/(\omega m_e)$  and to good accuracy can be neglected. One can see that in the region  $m_V^2 \ll \omega^2 |\Delta\epsilon_r|$ , the absorption rate of the  $T$  modes scales as  $m_V^4$ , whereas for the  $L$  mode, it is always proportional to  $m_V^2$ . In the opposite limit, Eq. (16) is given by the number density of atoms  $n_A$ ,  $\sigma_{\text{abs}}$ , and the velocity of dark photons  $v_V$ ,  $\Gamma_T = \kappa^2 \omega \text{Im}\epsilon_r = \kappa^2 n_A v_V^{-1} \sigma_{\text{abs}}$ . (We work in  $c = 1$  units.)

Going over to the HC, we take  $m_{h'} \sim m_V$  and consider the absorption process (5) in the limit of both masses being small. Using the equivalence to the scattering of charged scalars, we write the amplitude as

$$\mathcal{M} = e_{\text{eff}}(k_1 + k_2)^\mu \langle A_\mu, A_\nu \rangle \langle f | J_{\text{EM}}^\nu(q) | i \rangle, \quad (17)$$

where  $k_1$  and  $k_2$  are the four-momenta of the incoming and outgoing  $\phi$  particles and  $q = k_1 - k_2$ . Medium-corrected photon propagators  $\langle A_\mu, A_\nu \rangle$  in the Coulomb gauge are given by

$$\langle A^i, A^j \rangle = \frac{\delta^{ij} - \hat{q}^i \hat{q}^j}{q^2 - \Pi_T}, \quad \langle A^0, A^0 \rangle = \frac{q^2}{|\vec{q}|^2 (q^2 - \Pi_L)}, \quad (18)$$

where  $\hat{q} \equiv \vec{q}/|\vec{q}|$ . Following the same steps as in the SC, summing over all the possible excited atomic states in the medium, we get

$$\sum_f |\mathcal{M}|^2 \approx -8e_{\text{eff}}^2 \text{Im}\epsilon_r \frac{q^2 k_1^0 (k_1^0 - q^0)}{[q^2 + q^{02} \Delta\epsilon_r]^2}, \quad (19)$$

where terms with further suppression by  $\Delta\epsilon_r$  are omitted. The differential scattering rate with respect to the energy transfer to atoms  $q^0$  is given by

$$\frac{d\Gamma}{dq^0} \approx \frac{e_{\text{eff}}^2}{4\pi^2} \frac{k_1^0 - q^0}{k_1^0} \left[ \log \left( \frac{4k_1^0 (k_1^0 - q^0)}{(q^0)^2 |\Delta\epsilon_r|} \right) - 1 \right] \text{Im}\epsilon_r(q^0). \quad (20)$$

Notice that the collinear divergence is regularized by the in-medium modification of the photon propagator.

*Limits from direct detection.*—Having obtained both solar fluxes and the absorption rates of dark photons, we are ready to calculate the experimental event rate. In a given experiment, the expected number of signal events in the SC can be written as

$$N_{\text{exp}} = VT \int_{\omega_{\min}}^{\omega_{\max}} \frac{\omega d\omega}{|\vec{q}|} \left( \frac{d\Phi_T}{d\omega} \Gamma_T + \frac{d\Phi_L}{d\omega} \Gamma_L \right) \text{Br}, \quad (21)$$

where  $V$  and  $T$  are the fiducial volume and live time of the experiment, respectively, and  $\text{Br}$  is the branching ratio of the photoionization rate to the total absorption rate.

Since both  $\text{Re}\varepsilon_r$  and  $\text{Im}\varepsilon_r$  are proportional to the number density of atoms of the material  $n_A$ , in the small  $m_V$  limit,  $\Gamma_T \propto n_A^{-1}$ . As a result, low density materials are best suited for the detection of  $T$  modes. However, as discussed in Ref. [6], the major component of the dark photon flux from the Sun is longitudinal, and from Eq. (16) we have  $\Gamma_L \propto n_A$ . Therefore, the detection abilities are directly proportional to the total active mass inside the detector. Given the significant enhancement in the low-energy part of the solar dark photon spectrum (Fig. 1), a detector with a low-threshold energy of  $O(100)$  eV will have a clear advantage. To date, the only work that considers limits on dark photons from direct dark matter (DM) detection is by the HPGC Collaboration (Ref. [9]). However, it used incomplete calculations of the solar flux, and as we will show in the following, the low-energy ionization signals by the XENON10 [10] and CoGeNT [11,12] Collaborations yield far more stringent limits.

The XENON10 Collaboration has published a study on low-energy ionization events in Ref. [10]. With 12.1 eV

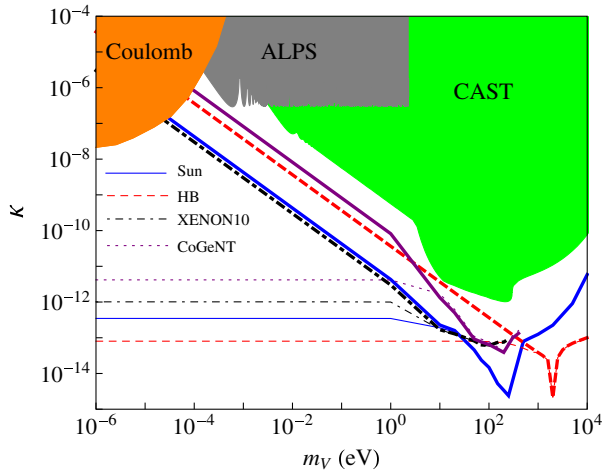


FIG. 2 (color online). Constraints on  $\kappa$  as functions of  $m_V$ . The solid, dashed, dot-dashed, and dotted curves show constraints from the energy loss of the Sun by requiring that the dark photon luminosity does not exceed 10% of the standard solar luminosity [17], energy loss in horizontal branch (HB) stars, the XENON10 experiment, and the CoGeNT experiment, respectively. The thick curves are for the SC, whereas the thin curves are for the HC with  $e' = 0.1$ . For comparison, the current bounds (gray shading) from the LSW-type experiments are shown (see Ref. [18] for details). The conservative constraint from the CAST experiment [19] by considering the contributions from only the transverse modes [4] is also shown in green shading. The orange shaded region is excluded from tests of the inverse square law of the Coulomb interaction [20].

ionization energy, the absorption of a dark photon with 300 eV energy can produce about 25 electrons. To get a conservative constraint, we count all the ionization events within a 20 keV nuclear recoil equivalent in Ref. [10], which corresponds to a signal of about 80 electrons. The total number of events is 246, which indicates a 90% C.L. upper limit on the detecting rate to be  $r < 19.3$  events  $\text{kg}^{-1} \text{day}^{-1}$  (similar to limits deduced in Ref. [13]). In the region  $12.1 \text{ eV} < \omega < 300 \text{ eV}$ , the ionization process dominates the absorption, and therefore  $\text{Br}$  in this region can be set to unity. The 90% C.L. upper limit on  $\kappa$  as a function of  $m_V$  is shown by the dot-dashed black curve in Fig. 2, where we can see that it gives the most stringent constraint in the SC. To arrive at these limits, we reconstruct  $\varepsilon_r$  for Xe from the real and imaginary parts of the refractive index of Xe. The imaginary part can be extracted from the total photoabsorption cross section [14,15], and the real part can be calculated from the imaginary part using the Kramers-Kronig dispersion relations. The improvement over other experimental probes is quite significant, considering that the signal scales as  $\kappa^4$ . We also collate the main constraints in Table I.

The published data from the CoGeNT DM experiment have a threshold of about 450 eV [12]. In this region, the dark photon flux from the Sun drops almost exponentially with energy, whereas the observed spectrum in CoGeNT is relatively flat. Therefore, in order to optimize the sensitivity, we only use the event counts in the interval 450–500 eV, and the 90% upper limit on the background subtracted rate is  $r < 0.6$  events  $\text{kg}^{-1} \text{day}^{-1}$ . The resulting sensitivity is shown as the thick dotted purple curve in Fig. 2, which is far weaker than the constraint from the energy loss of the Sun.

In the HC,  $N_{\text{exp}}$  in Eq. (21) must include a contribution from Eq. (20), and it dominates in the region  $m_V^2 \ll \omega^2 |\Delta\varepsilon_r|$  but is subdominant if  $m_V^2 \sim \omega^2 |\Delta\varepsilon_r|$ . Since the flux of  $V(h')$  in the HC is mainly contributed from the conversion of transverse photons in the Sun, the spectral distribution reflects the solar temperature (Fig. 1), with the cutoff above 1 keV. A dark photon of 1 keV energy can at most produce about 60 electrons in liquid xenon. For  $e' = 0.1$ , the 90% C.L. upper limit is shown as the thin dot-dashed curve in Fig. 2. For the sensitivity from CoGeNT, we take into account all the events from 450 eV to 1 keV, and the associated line is shown as the thin dotted curve in Fig. 2 and included in Table I as a limit on  $e_{\text{eff}}$ . In both the HC and the SC, CoGeNT does not have the sensitivity to constrain dark photons since the required flux is not supported by the Sun.

TABLE I. Sensitivities to  $\kappa$  and  $e_{\text{eff}}$  in the small  $m_V$  region.

Model parameters	Sun	HB	XENON10	CoGeNT
SC, $\kappa \times (m_V/\text{eV})$	$4 \times 10^{-12}$	$4 \times 10^{-11}$	$3 \times 10^{-12}$	$8 \times 10^{-11}$
HC, $e_{\text{eff}}$	$3 \times 10^{-14}$	$8 \times 10^{-15}$	$1 \times 10^{-13}$	$4 \times 10^{-13}$



*Conclusions.*—We point out that the unprecedented sensitivity of some of the DM experiments to ionization allows us to turn them into the most sensitive dark photon helioscopes. By directly calculating the ionization signal, we show that the ensuing constraint from the XENON10 experiment significantly surpasses any other bounds on dark photons, including very tight stellar energy loss constraints in the  $m_V$  interval from  $10^{-5}$  to 100 eV. In the case of “minicharged” particles (equivalent to the version of dark photons broken through the Higgs mechanism), we also derive a stringent bound  $e_{\text{eff}} < 10^{-13}$ , which is second only to the constraint from the energy loss of the horizontal branch stars; see also Ref. [16]. Given the enormous amount of experimental progress in the field of direct DM detection, one can be optimistic that future sensitivity to dark photons and other light particles is bound to be further improved.

We acknowledge useful correspondence with G. Raffelt and J. Redondo on stellar production rates and the strength of the solar luminosity constraint. Research at the Perimeter Institute is supported in part by the Government of Canada through NSERC and by the Province of Ontario through MEDT.

- 
- [1] B. Holdom, *Phys. Lett.* **166B**, 196 (1986); L. B. Okun, *Sov. Phys. JETP* **56**, 502 (1982) [*Zh. Eksp. Teor. Fiz.* **83**, 892 (1982)].
  - [2] J. Jaeckel and A. Ringwald, *Annu. Rev. Nucl. Part. Sci.* **60**, 405 (2010).
  - [3] M. Ahlers, H. Gies, J. Jaeckel, J. Redondo, and A. Ringwald, *Phys. Rev. D* **77**, 095001 (2008).
  - [4] J. Redondo, *J. Cosmol. Astropart. Phys.* **07** (2008) 008.
  - [5] G. G. Raffelt, *The Astrophysics of Neutrinos, Axions, and Other Weakly Interacting Particles* (University of Chicago Press, Chicago, 1996), p. 664.
  - [6] H. An, M. Pospelov, and J. Pradler, [arXiv:1302.3884](#).
  - [7] S. Davidson, B. Campbell, and D. C. Bailey, *Phys. Rev. D* **43**, 2314 (1991); S. Davidson, S. Hannestad, and G. Raffelt, *J. High Energy Phys.* **05** (2000) 003.
  - [8] C. Itzykson and J.-B. Zuber, *Quantum Field Theory* (McGraw-Hill, New York, 1980).
  - [9] R. Horvat, D. Kekez, M. Krcmar, Z. Krecak, and A. Ljubcic, [arXiv:1210.1043](#).
  - [10] J. Angle *et al.* (XENON10 Collaboration), *Phys. Rev. Lett.* **107**, 051301 (2011).
  - [11] C. E. Aalseth *et al.*, *Phys. Rev. Lett.* **107**, 141301 (2011).
  - [12] C. E. Aalseth *et al.* (CoGeNT Collaboration), *Phys. Rev. Lett.* **106**, 131301 (2011).
  - [13] R. Essig, A. Manalaysay, J. Mardon, P. Sorensen, and T. Volansky, *Phys. Rev. Lett.* **109**, 021301 (2012).
  - [14] B. L. Henke, E. M. Gullikson, and J. C. Davis, *At. Data Nucl. Data Tables* **54**, 181 (1993).
  - [15] W. F. Chan, G. Cooper, X. Guo, G. R. Burton, and C. E. Brion, *Phys. Rev. A* **46**, 149 (1992).
  - [16] M. Ahlers, J. Jaeckel, J. Redondo, and A. Ringwald, *Phys. Rev. D* **78**, 075005 (2008).
  - [17] P. Gondolo and G. G. Raffelt, *Phys. Rev. D* **79**, 107301 (2009).
  - [18] K. Ehret *et al.*, *Phys. Lett. B* **689**, 149 (2010).
  - [19] S. Andriamonje *et al.* (CAST Collaboration), *J. Cosmol. Astropart. Phys.* **04** (2007) 010.
  - [20] D. F. Bartlett and S. Lögl, *Phys. Rev. Lett.* **61**, 2285 (1988).